Available online at www.sciencedirect.com
ScienceDirect
Journal of Molecular and Cellular Cardiology 41 (2006) 807–815
Journal of Molecular and Cellular Cardiology
www.elsevier.com/locate/yjmcc

Original article

Endothelin-1 induced hypertrophic effect in neonatal rat cardiomyocytes: Involvement of Na^+/H^+ and Na^+/Ca^{2+} exchangers

Raúl A. Dulce [a], Cecilia Hurtado [c], Irene L. Ennis [a], Carolina D. Garciarena [a], María C. Alvarez [a], Claudia Caldiz [a], Grant N. Pierce [c], Enrique L. Portiansky [b], Gladys E. Chiappe de Cingolani [a], María C. Camilión de Hurtado [a,*]

[a] *Centro de Investigaciones Cardiovasculares, Facultad de Ciencias Médicas, UNLP, 60 y 120, 1900, La Plata, Argentina*
[b] *Facultad de Ciencias Veterinarias, UNLP, Argentina*
[c] *Division of Stroke and Vascular Disease, St. Boniface Hospital Research Center, Manitoba, Canada*

Received 29 December 2005; received in revised form 19 April 2006; accepted 17 May 2006
Available online 21 July 2006

Abstract

Endothelin-1 (ET-1) is a potent agonist of cell growth that also stimulates Na^+/H^+ exchanger isoform 1 (NHE-1) activity. It was hypothesized that the increase in intracellular Na^+ ($[Na^+]_i$) mediated by NHE-1 activity may induce the reverse mode of Na^+/Ca^{2+} exchanger (NCX_{rev}) increasing intracellular Ca^{2+} ($[Ca^{2+}]_i$) which in turn will induce hypertrophy. The objective of this work was to test whether the inhibition of NHE-1 or NCX_{rev} prevents ET-1 induced hypertrophy in neonatal rat cardiomyocytes (NRVMs). NRVMs were cultured (24 h) in the absence (control) and presence of 5 nmol/L ET-1 alone, or combined with 1 μmol/L HOE 642 or 5 μmol/L KB-R7943. Cell surface area, ^{3}H-phenylalanine incorporation and atrial natriuretic factor (ANF) mRNA expression were increased to 131 ± 3, 220 ± 12 and 190 ± 25% of control, respectively ($P < 0.05$) by ET-1. $[Na^+]_i$ and total $[Ca^{2+}]_i$ were higher (8.1 ± 1.2 mmol/L and 636 ± 117 nmol/L, respectively) in ET-1-treated than in control NRVMs (4.2 ± 1.3 and 346 ± 85, respectively, $P < 0.05$), effects that were cancelled by NHE-1 inhibition with HOE 642. The rise in $[Ca^{2+}]_i$ induced by extracellular Na^+ removal (NCX_{rev}) was higher in ET-1-treated than in control NRVMs and the effect was prevented by co-treatment with HOE 642 or KB-R7943 (NCX_{rev} inhibitor). The ET-1-induced increase in cell area, ANF mRNA expression and ^{3}H-phenylalanine incorporation in ET-1-treated NRVM were decreased by NHE-1 or NCX_{rev} inhibition. Our results provide the first evidence that NCX_{rev} is, secondarily to NHE-1 activation, involved in ET-1-induced hypertrophy in NRVMs.

Keywords: Endothelin-1; Na^+/H^+ exchanger; Na^+/Ca^{2+} exchanger; Intracellular Na^+; Cardiac hypertrophy

1. Introduction

Cardiac hypertrophy (CH) is triggered by several physiological and pathological conditions that cause an increase in hemodynamic load. Although the process may have a beneficial effect at the beginning, epidemiological studies indicate that chronic CH is associated with an increase in cardiovascular morbidity/mortality risk [1]. Therefore, elucidation of the signaling pathways leading to CH will have significant implications for the development of therapeutic strategies.

Locally produced angiotensin II (Ang II) and endothelin-1 (ET-1) are involved in the hypertrophic response to hemodynamic overload [2–4]. They trigger a complex set of intracellular signals leading to the activation of the fetal gene program, increase in cell size, protein synthesis and sarcomere assembly, which constitute consistent markers of CH. Although the process has received considerable attention, it is not completely understood. One common downstream effector of ET-1 and Ang II is the Na^+/H^+ exchanger isoform 1 (NHE-1) [5–7] which is known to participate in CH development [8,9]. Our work hypothesis was that the rise in $[Na^+]_i$ achieved through NHE-1 activation may promote the operation of the Na^+/Ca^{2+} exchanger (NCX) in reverse mode allowing Na^+_i to be exchanged for Ca^{2+}_o thereby increasing $[Ca^{2+}]_i$ levels. $[Ca^{2+}]_i$

* Corresponding author. Fax: +54 221 483 4833.
E-mail address: mariacam@atlas.med.unlp.edu.ar (M.C. Camilión de Hurtado).

0022-2828/$ – see front matter © 2006 Published by Elsevier Inc.
doi:10.1016/j.yjmcc.2006.05.016

is an important regulatory point for cell growth, but the mechanism underlying the elevation of $[Ca^{2+}]_i$ in response to hypertrophic stimuli is still unresolved. The coupling of the NHE-1 stimulation with the NCX operating in reverse mode (NCX_{rev}) has been shown to be responsible for the positive inotropic effect of ET-1 in adult myocardium [10]. The objective of the present study was to explore whether a similar coupled pathway accounts for ET-1-induced hypertrophy in neonatal rat ventricular myocytes (NRVMs).

2. Materials and methods

Experiments were conducted in accordance with the Guide for the Care and Use of Laboratory Animals (NIH Publication No. 85-23, 1996) on cultured NRVM isolated from 2 to 3-day-old Wistar rats as previously described [11]. Briefly, 15–20 hearts were digested with phosphate buffer saline (PBS) with 55 mmol/L glucose (PBS/glucose), 740 units of collagenase II, 370 units of trypsin I and 2880 units of DNAse I (all from Whortington). Cells were filtered through 100 μm mesh, spun at 2000 rpm for 5 min and were then run through a Percoll (Amersham) gradient to separate cardiomyocytes from other cell types. Cardiomyoctes were washed with F-10 media and incubated for 24 h under humidified air with 5% CO_2 at 37 °C, in F-10 media containing 10% fetal bovine serum (FBS), 10% horse serum, 10 μmol/L cytosine β-D-arabinofuresamide, 100 units/mL penicillin and 100 μg/mL streptomycin (all from Invitrogen). The next day, the cell medium was replaced by DMEM (Gibco) containing 1% FBS, 20 nmol/L selenium, 10 μg/mL insulin, 10 μg/mL transferrin, 2 mg/mL bovine serum albumine, 10 μmol/L cytosine β-D-arabinofuresamide and 20 μg/mL ascorbic acid and incubated for another 24 h. Following this, the medium was replaced with serum-free DMEM and cardiomyocytes were incubated for an additional 24 h before being used under the different experimental conditions. NRVMs were plated at a density of $10^5/cm^2$ except for cell area measurements where density was reduced to $5 \times 10^4/cm^2$ to obtain individually plated cells. Except otherwise specified, all reagents used in this study were from Sigma-Aldrich.

2.1. Experimental protocol

Serum-starved NRVMs were cultured for 24 h in control condition or treated with: 5 nmol/L ET-1 alone; ET-1 combined with one of the following: 1 μmol/L HOE 642 (NHE-1 inhibitor, Aventis Pharma), 5 μmol/L KB-R7943 (selective NCX_{rev} inhibitor, Tocris), 1 μmol/L TAK 044 (mixed ET_A/ET_B receptor antagonist, Takeda Pharmaceutical Co.) or 300 nmol/L BQ123 (selective ET_A receptor antagonist). In the experiments with receptor antagonists or inhibitory drugs, they were added 15 min before ET-1 addition. Parallel cultures with TAK 044, HOE 642, KB-R7943 or dimethylmethoxi sulfonic acid (DMSO) were also performed. All compounds were dissolved in distilled water with the exception of KB-R7943 which was dissolved in DMSO.

2.2. Incorporation of [^{3}H] phenylalanine

The extent of de novo protein synthesis was estimated by [^{3}H] phenylalanine incorporation in NRVM grown in collagen-coated multiwells. NRVM were incubated in duplicate with L-[2,3,4,5,6-^{3}H] phenylalanine (10 μCi/mL, Amersham Biosciences) according to the experimental protocols described above. The cells were thoroughly washed with ice-cold PBS (pH 7.4) and 10% trichloroacetic acid (TCA) was added at 4 °C for 60 min to precipitate protein. Each well was then scraped and the precipitate washed twice with 10% TCA and twice with 95% ethanol. Between washes with TCA, the suspension was briefly sonicated to improve the washing procedure. Finally, the pellet was suspended in 0.15 mol/L NaOH. Aliquots were counted by a scintillation counter and the results expressed as nanomoles of [^{3}H] phenylalanine incorporated per disc. DNA content/disc was fluorometrically determined in neutralized samples with the fluorescent dye bisbenzimide (Hoecht 33258).

2.3. Western blot immunoanalysis

Incubation medium was removed and myocytes were washed twice with cold PBS and lysed with RIPA buffer containing (in mmol/L) 50 Tris, 150 NaCl, 1 EDTA, 1 EGTA, 1% Triton X 100, 0.5% sodium deoxycholate, pH 7.5 with protease inhibitors. The samples were kept on ice for 30 min and centrifuged at 14,000 rpm at 4 °C for 12 min. The supernatant was kept at −80 °C until used. NRVM membranes were denatured and equal amounts of protein (45 μg/lane) were subjected to 7% PAGE. Immunoblot analysis was performed with rabbit polyclonal antibody for NHE-1 (kindly provided by Dr. Donowitz, The Johns Hopkins University, Baltimore, MD). NCX protein was measured with a monoclonal antibody (MAB-1590, Chemicon). Immunodetection of the primary antibodies was carried out with peroxidase-conjugated secondary antibodies and enhanced chemiluminiscence reaction system (Amersham Biosciences). Densitometric analysis of NHE-1 and NCX proteins was referred to those of actin.

2.4. Isolation of total RNA and real-time PCR

Quantitative PCR to measure ANF expression was performed using the real-time SYBR Green PCR method. Total RNA was isolated using RNeasy Mini Kit and RNase free Dnase Set (Qiagen) and reverse-transcribed using Omniscript RT Kit (Qiagen) as previously described [12]. The primers were designed using Primer3 software based on published sequences: GAPDH forward primer 5′-GGGTGTGAACCACGAGAAAT-3′, reverse primer 5′-CCACAGTCTTCTGAGTGGCA-3′; ANF forward primer 5′-AGGGCTTCTTCCTCTTCCTG-3′, reverse primer 5-TCCAGGTGGTCTAGCAGGTT-3′.

2.5. Measurement of cell area

At the end of treatment, NVRMs were washed twice with PBS/glucose and fixed in buffered 10% formaldehyde. Cell

surface area (CSA) was determined in no less than 50 randomly selected cells with visible rounded nucleous per experiment. The images were captured using an analog video camera, digitized and processed by a computer morphometry program (Image-Pro Plus for Windows 95/98 v4.5-Media Cybernetics, Silver Spring, MA, USA) by an observer unaware of the treatment protocol.

2.6. Determination of intracellular pH (pH_i), $[Na^+]_i$ and $[Ca^{2+}]_i$ levels

Confluent NRVMs grown on collagen-coated coverslips and placed in a cell chamber on the stage of an inverted microscope (TE2000-U Nikon) were used to measure pH_i, $[Ca^{2+}]_i$ and $[Na^+]_i$ by microepifluorescence. One coverslip under the different experimental conditions was used for each experiment. NRVMs were loaded with BCECF, Fura-2 or SBFI (AM forms, Molecular Probes) for 20 (the former 2 dyes) or 60 (the latter) min, respectively, followed by 3 washes with dye-free solution and incubation for another 20 min to allow for dye de-esterification. In NRVMs exposed to agonist/blockers, this condition was maintained throughout the entire loading/washout and experimental protocols. Even though NRVMs beat at a similar spontaneous rate (see Results), all the determinations were carried out in electrically paced (0.5 Hz, starting 5 min prior to begin the fluorescence records) preparations at room temperature. Emitted fluorescence was monitored at 535 (BCECFand SBFI) or 510 nm (Fura-2) with excitation wavelengths alternating 440/485 (BCECF) or 360/380 nm for SFBI and Fura-2. The excitation filters rotation and fluorescence recording were achieved with an IonOptix Fluorescence System coupled to the microscope. The ratio (R) of emitted fluorescence signals was performed off-line after subtraction of the corresponding autofluorescence value at each wavelength. R values were transformed into pH_i, Na^+ or Ca^{2+} values using "in vivo" calibration curves. BCECF fluorescence was calibrated by the high-K^+ nigericin method previously described [10] and that of SBFI was made according to Harootunian et al. [13] with 2.0 μmol/L gramicidin, 5.0 μmol/L monensin and 0.05 mmol/L ouabain. Appropriate mixtures of 150 mmol/L Na^+-0 K^+ and 150 mmol/L K^+-0 Na^+ solutions were made to obtain different Na^+ concentrations within the physiological range (4 to 16 mmol/L). Fura-2 was calibrated with a solution containing (in mmol/L), 140 KCl, 1.2 $MgCl_2$, 10 HEPES (pH 7.4, NaOH) 4 NaCN, 2 iodoacetate and 0.01 ionomycin. Different $[Ca^{2+}]$ covering the most relevant $[Ca^{2+}]_i$ range were obtained by mixing in various proportions the zero (10 mmol/L EGTA) and saturating (10 mmol/L CaEGTA) $[Ca^{2+}]$ solutions. $[Ca^{2+}]_i$ was calculated using the following equation [14]:

$$[Ca^{2+}]_i = K'_d(R - R_{min})/(R_{max} - R)$$

where K'_d is the apparent dissociation constant for Fura-2 under our experimental conditions of in vivo calibrations. No significant difference was observed between calibration curves obtained with control or hypertrophied NRVMs. The calculated average K_d, R_{min} and R_{max} values were 370 nmol/L, 0.21 and 1.06, respectively.

2.7. Determination of NHE-1 activity

The rate of acid efflux (J_{H+}) during the recovery from an imposed acid intracellular load was used as the index of NHE-1 activity. For this, NRVMs were transiently exposed (4 min) to 20 mmol/L NH_4Cl and its subsequent washout. Rapid solution changes, whenever required, were made using mini solenoid valves located close to the cell chamber inlet. J_{H+} was calculated from the equation $J_{H+} = \beta_i \times dpH_i/dt$, where β_i is the intrinsic cell buffer capacity and dpH_i/dt is the rate of recovery estimated as the derivative of the exponential fit of pH_i vs. time records. β_i was estimated from Δbase / ΔpH_i caused by the NH_4Cl washout.

2.8. Caffeine pulses

They were performed according to a similar protocol to the one described by Bassani et al. [15]. Fura-2 loaded NRVMs were paced for 15 min and electrical stimulation was stopped 15 s before rapidly switching to a HEPES buffer containing 10 mmol/L caffeine.

2.9. Induction of NCX_{rev}

Fura-2 loaded cardiomyocytes were subjected to abrupt extracellular Na^+ removal (Na^+_o) by equimolar substitution of Li^+ for Na^+ in the superfusate.

2.10. Statistics analysis

All results are presented as mean ± standard errors (SE). Statistical difference between groups was assessed by ANOVA with Newman–Keuls post test. $P < 0.05$ was considered statistically significant.

3. Results

3.1. ET-1-induced hypertrophy in NRVMs

Cultured NRVMs showed spontaneous beating activity that was not changed by the treatment protocols (Table 1). The hypertrophic effect of ET-1 was evaluated by the increase in cell surface area (CSA), ^{3}H-phenylalanine incorporation, total protein content and ANF mRNA expression. In ET-1-stimulated NRVMs, CSA was 131 ± 3% of control (n = 325 each, Figs. 1A–B). The effect was abrogated by the mixed $ET_{A/B}$ receptor antagonist TAK-044 but not by BQ123 (n = 200 each, Figs. 1A–B). Data regarding the ability of the specific ET_A receptor blocker BQ123 to antagonize the hypertrophic effect of ET-1 are controversial. While some studies showed complete inhibition [3,16], other authors found both ET_A and ET_B receptor subtypes to be implicated in ET-1-induced CH [17]. In addition, partial agonist activity has been attributed to BQ123 [18]. ANF mRNA expression increased to 190 ± 25% of control

Table 1
DNA content and spontaneous beating rate values in the different experimental groups

Control	ET-1	ET + HOE	ET + KBR	HOE	KBR	ET + TAK
DNA content (μg/disc)						
1.23 ± 0.15 (n = 8)	1.36 ± 0.13 (n = 8)	1.35 ± 0.15 (n = 4)	1.30 ± 0.09 (n = 7)	1.35 ± 0.14 (n = 4)	1.22 ± 0.12 (n = 7)	1.19 ± 0.12 (n = 4)
Beats/min						
33 ± 3 (n = 4)	34 ± 9 (n = 4)	26 ± 5 (n = 4)	27 ± 8 (n = 3)			

in NRVM exposed to ET-1 and this effect was sensitive to ET-receptors blockade with TAK 044 (Fig. 1C).

In ET-1-treated NRVMs, ^{3}H-phenylalanine incorporation was about twice the control value (9.49 ± 1.30 vs. 4.45 ± 0.71 nmol/disc, respectively, n = 12 each, $P < 0.05$). The effect of ET-1 on ^{3}H-phenylalanine incorporation was prevented by TAK 044 (5.09 ± 1.49 nmol/disc, n = 5). The overall data in percentage of control value are shown in Fig. 1C. Under each experimental condition, total protein content paralleled the increase in ^{3}H-phenylalanine incorporation implying a direct relationship between both parameters (Fig. 1D). Total DNA content was not altered by any treatment (Table 1).

3.2. $[Na^+]_i$ level in hypertrophied NRVMs

The level of $[Na^+]_i$ was higher in ET-1-treated than in control NRVMs (8.1 ± 1.2 vs. 4.2 ± 1.3 mmol/L, n = 4, $P < 0.05$, Fig. 2A). The rise in $[Na^+]_i$ was prevented by either the blockade of ET receptors (4.2 ± 0.5 mmol/L, n = 4) or NHE-1 inhibition (4.9 ± 1.4 mmol/L, n = 4). These results strongly suggested that the elevation of $[Na^+]_i$ in hypertrophied NRVMs could have been caused by a stimulatory effect of ET-1 on NHE-1 activity. This possibility was explored assessing the pH_i recovery from an intracellular acid load. Fig. 2B shows the pH_i vs. time records during the recovery phase of a representative experiment carried on control and ET-1-treated NRVMs. A faster return to steady pH_i value was observed in ET-1-treated than in control NRVMs. Actual NHE-1 activity is usually expressed in terms of J_{H+} and the estimated average values at the beginning of the pH_i recovery are also shown in Fig. 2B. J_{H+} was larger in ET-1-treated compared with control NRVMs. Since NHE-1 protein expression was similar (n = 5, Fig. 2C) in ET-1-treated and control cells, it can be speculated that the increase in NHE-1 activity in hypertrophied NRVMs resulted from an ET-1-induced increase in the exchanger turnover rate.

3.3. NCX activity and $[Ca^{2+}]_i$ in hypertrophied NRVMs

An increase in $[Na^+]_i$ would shift the balance of NCX fluxes to favor less Ca^{2+} efflux (forward mode) and/or more Ca^{2+} influx (reverse mode) resulting in increased $[Ca^{2+}]_i$. The former possibility was explored comparing caffeine-induced Ca^{2+} transient in ET-1-treated myocytes vs. control. Fig. 3A shows representative experiments of this type. The peak of caffeine-evoked Ca^{2+} transients is related to the sarcoplasmic reticulum (SR) content while the decline mainly results from Ca^{2+} extrusion by NCX activity and to a lesser extent to sarcolemmal Ca^{2+} ATPase activity and organelle sequestration. Consistent with the sparse and immature SR development in NRVMs [19], the peak of caffeine-evoked Ca^{2+} transients was lower than

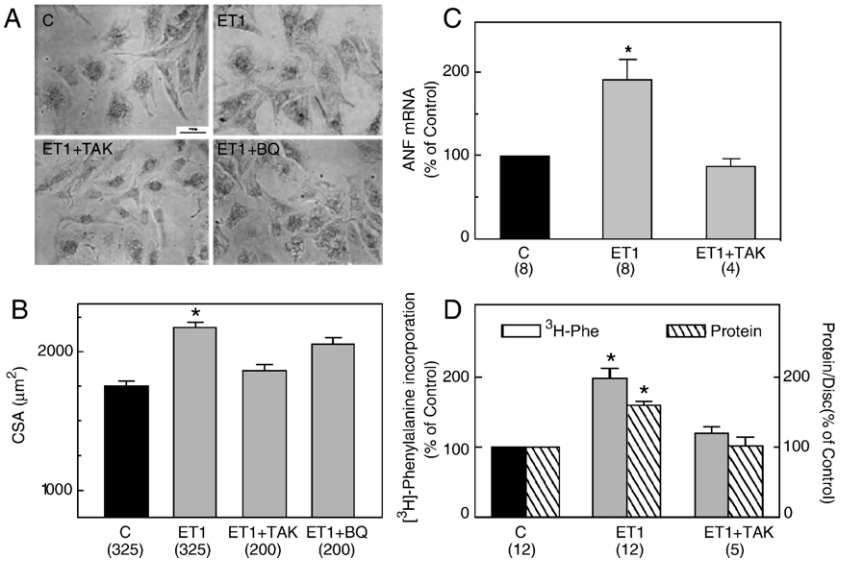

Fig. 1. Cardiomyocyte hypertrophy induced by ET-1. (A) Microphotographs of cultured NRVM in absence (C) or presence of 5.0 nmol/L ET-1 alone (ET1), or combined with 1 μmol/L TAK 044 (ET1 + TAK) or 300 nmol/L BQ123 (ET1 + BQ); scale bar indicates 50 μm. (B) Cell surface area (CSA) of the abovementioned groups. (C) ANF mRNA expression. (D) ^{3}H-phenylalanine incorporation and total protein content for the specified groups. Numbers of determinations are indicated in parentheses. *$P < 0.05$ vs. C, ANOVA.

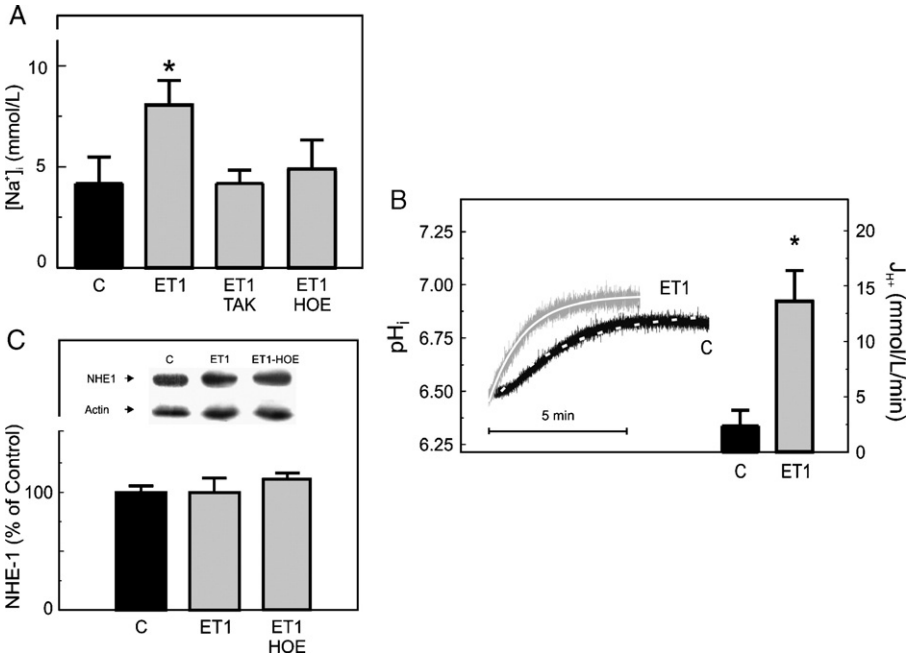

Fig. 2. ET-1-induced elevation of $[Na^+]_i$ in hypertrophied NRVMs is dependent on NHE-1 activity. (A) Average values of $[Na^+]_i$ in the designated experimental groups ($n = 4$, from separate isolation procedure each). (B) Representative records of the pH_i recovery phase from an intracellular imposed acid load using the NH_4Cl prepulse technique in control (black trace) and ET-1-treaded-NRVMs (gray trace). The exponential fit of pH_i vs. time records is shown superimposed in white. Bars on the right show the initial rate of net acid efflux (J_{H+}). (C) NHE-1 protein expression by immunoblot assay ($n = 3$, from separate isolation procedure each). *$P < 0.05$ vs. all other groups, ANOVA.

those during electrically induced twitches (Tw) in both control and ET-treated NRVMs (37 ± 8 and 40 ± 14%, $n = 5$, respectively). Also, the rate of rise and relaxation of caffeine-evoked Ca^{2+} transients was slower than during regular twitches as expected in cells with disabled SR. ET-1 did not modify the rate of caffeine-evoked Ca^{2+} transients relaxation as denoted by the time-course of the $[Ca^{2+}]_i$ decline shown in Fig. 3B and the respective Tau values (4.62 ± 1.29 and 3.52 ± 0.77 s, $n = 5$ in control and ET-1-treated NRVMs, respectively), suggesting that forward mode of NCX was not affected by the peptide.

To assess whether the increase in $[Na^+]_i$ would favor more Ca^{2+} influx through NCX_{rev}, the increase in $[Ca^{2+}]_i$ induced by sudden extracellular Na^+ removal was compared in control and ET-1-treated NRVMs. Fig. 3C illustrates a representative experiment. The increase in $[Ca^{2+}]_i$ carried by NCX_{rev} after Na^+_o removal was larger in ET-1-treated than in control NRVMs. In the former, $[Ca^{2+}]_i$ increased to 2345 ± 446 nmol/L whereas it raised to 1149 ± 302 nmol/L in control NRVMs (Fig. 3D, $P < 0.05$). Since NCX protein expression did not change (Fig. 3F), the results indicate that the larger $[Ca^{2+}]$ influx carried by NCX_{rev} in ET-1-treated NRVMs might be ascribed to an increase in driving force.

Obviously, extracellular Na^+ deprivation is non-physiologic but during the course of an action potential (AP) a similar condition of changes in NCX driving force that favors NCX_{rev} mode may well occur [20]. Therefore, the equilibrium potential for the exchange (E_{NCX}) was calculated[1] to estimate whether NCX_{rev} may contribute to Ca^{2+} entry during the spontaneous contractions of cultured control and ET-1-treated NRVM. The results obtained are shown in Fig. 3E which illustrates how E_{NCX} may be expected to change during the course of a theoretical NRVM's AP [11]. During diastole, E_{NCX} will be close to 10 mV considering the mean $[Na^+]_i$ and diastolic $[Ca^{2+}]_i$ values determined in control NRVMs (Na^+_o and Ca^{2+}_o were 137 and 2.38 mmol/L, respectively). Thus, at a resting V_m of ~−70 mV, $E_{NCX} > V_m$ during diastole and Ca^{2+} extrusion through NCX (forward mode) would be thermodynamically favored. E_{NCX} increases during the AP due to the increase in $[Ca^{2+}]_i$ transient (considering cytosolic $[Na^+]_i$ stable). The decrease in V_m during the upstroke, turns $V_m > E_{NCX}$ for a short period, whose actual duration depends on the relative V_m and E_{NCX} values. During this period (shaded area), Ca^{2+} entry through NCX_{rev} is favored. When E_{NCX} was computed considering the average $[Na^+]_i$ and $[Ca^{2+}]_i$ transient determined in ET-1-treated NRVMs, the calculated values were lower than in control (mostly due to the higher $[Na^+]_i$ level). Consequently, the period during which $V_m > E_{NCX}$ (NCX_{rev} favored) was greatly extended.

Representative $[Ca^{2+}]_i$ transients during electrically induced twitches in both control and ET-1-treated NRVMs can be appreciated in Fig. 3A and at the beginning of the tracings shown in Fig. 3C. Diastolic $[Ca^{2+}]_i$ level was somewhat higher in ET-1-treated NRVMs but the difference with control did not reach the level of significance (205 ± 47, $n = 9$ vs. 117 ± 44 nmol/L, $n = 11$, respectively). Neither peak systolic $[Ca^{2+}]_i$ during the twitch was significantly modified by ET-1, although it showed a similar trend. On average, peak systolic

[1] E_{NCX} was calculated as $E_{NCX} = 3E_{Na} - E_{Ca}$, considering a stoichiometry of 3Na:1Ca [18].

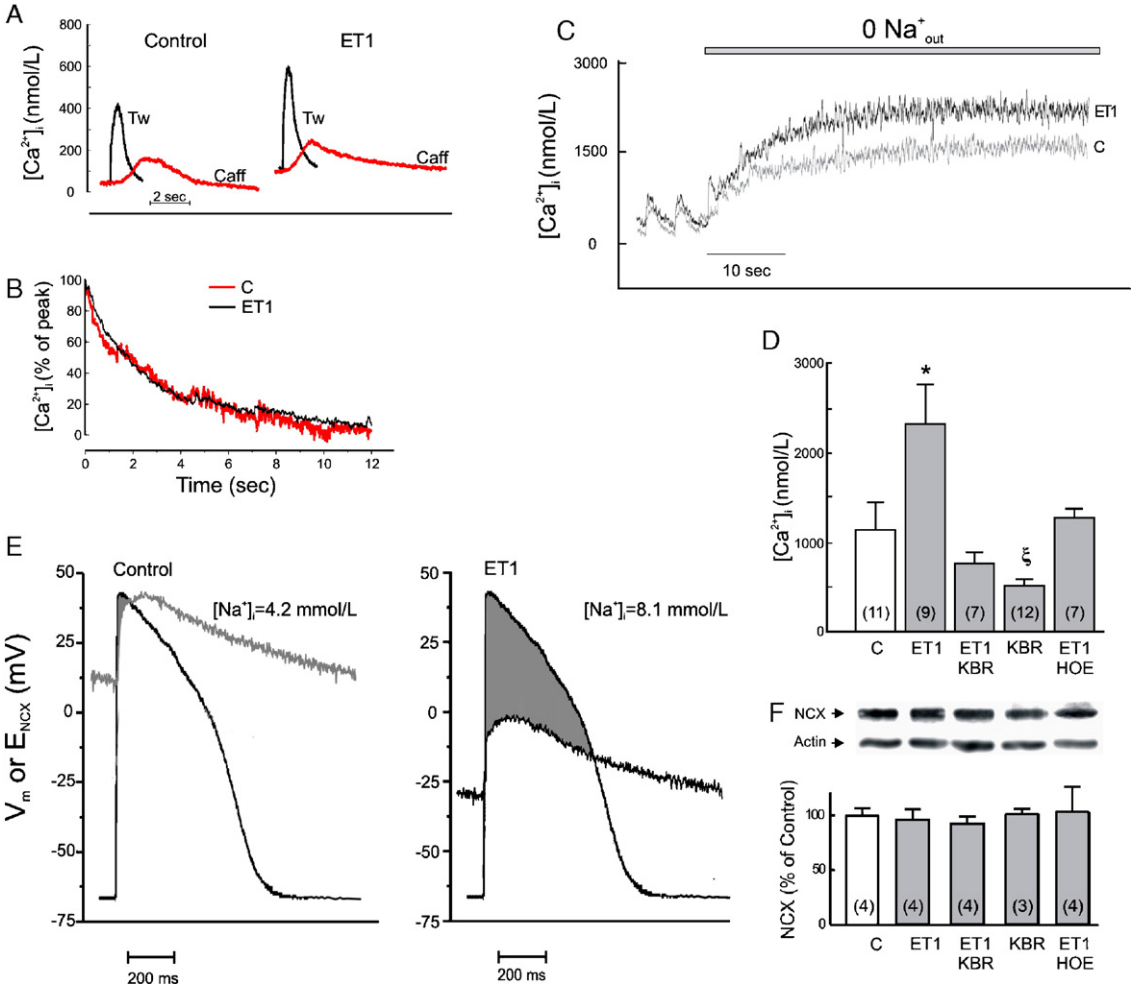

Fig. 3. NCX_{rev} is favored in ET-1-treated NRVMs. (A) Representative records of $[Ca^{2+}]_i$ transients evoked by electrical pacing (Tw) or caffeine pulse (Caff) in control and ET-1-treated NRVMs. (B) Average relaxation time-course of caffeine-evoked $[Ca^{2+}]_i$ transients in percent of maximum in control and ET-1-treated NRVMs ($n = 5$ each). (C) Representative traces showing the effect of removing Na^+_o on $[Ca^{2+}]_i$ in control (gray trace) and ET-1-treated NRVM (black trace). (D) Average maximum $[Ca^{2+}]_i$ attained during Na^+_o removal under the specified experimental conditions. (E) Schematic diagram of the estimated changes in E_{NCX} during a theoretical action potential (AP) in control and ET-1-treated NVRM. To compute E_{NCX} values, $[Ca^{2+}]_o = 2.38$ mM and $[Na^+]_o = 137$ mmol/L and averaged $[Na^+]_i$ and $[Ca^{2+}]_i$ transients values as actually measured under both experimental conditions were used assuming an exchange stoichiometry of 3Na:1Ca. V_m values correspond to a theoretical AP from a control NVRMs,[11] and, for simplicity, it was assumed to be the same for both conditions. When $V_m > E_{NCX}$, Ca^{2+} influx through NCX_{rev} is thermodynamically favored (shaded areas). (F) NCX protein expression by immunoblot assay under the specified conditions. Numbers of determinations from separate experiments are indicated in parentheses. *$P < 0.05$ vs. all other groups; $^{i}P < 0.05$ vs. C, ANOVA.

$[Ca^{2+}]_i$ reached to 400 ± 90 in control and 515 ± 108 nmol/L in ET-1-treated NRVMs. However, total cytosolic Ca^{2+} as assessed by integrating the area under the $[Ca^{2+}]_i$ vs. time curve during the contractile cycle was increased in ET-1-treated NRVMs compared to controls (636 ± 117 vs. 346 ± 85 nmol/L/cycle, respectively, $P < 0.05$).

Next the effect of NCX_{rev} inhibition with KB-R7943 was studied. NRVMs exposed to 5 μmol/L KB-R7943 showed a decrease in the maximal $[Ca^{2+}]_i$ rise after Na^+_o removal (Fig. 3D) compared to controls without changing diastolic $[Ca^{2+}]_i$ value (158 ± 24 nmol/L, $n = 12$), thus indicating a reduction in Ca^{2+} entry through NCX_{rev}. In comparison with control NRVMs, this reduction amounted to 63 ± 7%, $n = 12$, $P < 0.05$. Although pilot experiments showed that 10 μmol/L KB-R7943 almost canceled NCX_{rev} operation (reduction of Ca^{2+} entry was 82 ± 16% of control with 10 μmol/L KB-R7943, $n = 5$), the concentration of 5 μmol/L KB-R7943 was selected for the experiments shown here to prevent effects that a higher dose may induce on other ion currents [21]. When KB-R7943 was applied to NRVMs before ET-1 treatment, ET-1-induced increase in Ca^{2+} entry through NCX_{rev} was suppressed (Fig. 3D). Also the increase in total cytosolic Ca^{2+} was cancelled when NRVMs were pretreated with KB-R7943 before ET-1. In these cells, total cytosolic Ca^{2+} was 326 ± 27 nmol/L/cycle (NS compared to control). Similar effect was produced by NHE-1 inhibition (Fig. 3D). Since diastolic $[Ca^{2+}]_i$ did not change (100 ± 14 nmol/L, $n = 7$), it might be assumed that NHE-1 inhibition prevented the increase in Ca^{2+} entry through NCX_{rev} as well as it prevented ET-1-induced rise in $[Na^+]_i$. Total cytosolic Ca^{2+} was not different from control in ET-1 plus HOE 642-treated NRVMs (315 ± 57 nmol/L/cycle). No change in NCX protein expression was produced by any of the pharmacological interventions (Fig. 3F).

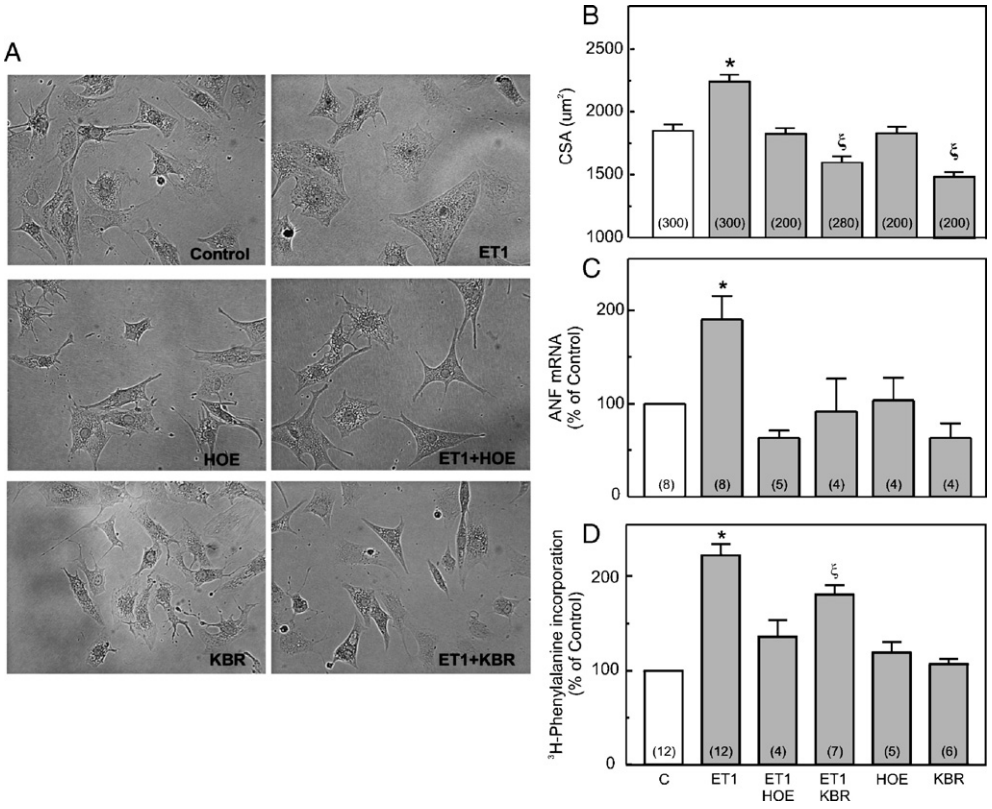

Fig. 4. Effect of NHE-1 or NCX_{rev} inhibition on the hypertrophic effect of ET-1 in NRVMs. (A) Microphotographs of cultured NRVMs under the specified experimental conditions. (B) Average cell surface area; (C) ANF mRNA expression of the same experimental groups and (D) ^{3}H-phenylalanine incorporation. Numbers of determinations are indicated between parentheses. *$P < 0.05$ vs. all other groups; $^{i}P < 0.05$ vs. C.

3.4. Effect of NHE-1 and NCX_{rev} inhibition on ET-1-induced hypertrophy in NRVMs.

Both NHE-1 and NCX inhibition suppressed the increase in CSA and ANF mRNA expression (Figs. 4A–C) and significantly reduced ^{3}H-phenylalanine incorporation (Fig. 4D) induced by ET-1 in NRVMs. CSA was reduced in NRVMs treated with KB-R7943 alone compared to the control group (Figs. 4A–B). A similar effect was produced by the solvent of KB-R7943 (DMSO). However, neither KBR alone nor DMSO modified ^{3}H-phenylanine incorporation or ANF mRNA expression (Figs. 4C–D; 107 ± 5 and 127 ± 21%, $n = 5$, respectively).

4. Discussion

CH occurs in response to numerous physiological and pathophysiological stimuli and the signaling pathways involved in the process are very complex. We showed herein an increase in NCX_{rev} in ET-1-treated NRVMs and that the hypertrophic action of the peptide was dampened by limiting the operation of NCX_{rev} with KB-R7943. We also showed that increased NCX_{rev} in ET-1-treated NRVM was linked to a rise in $[Na^+]_i$ mediated by higher NHE-1 activity. Of importance, the changes in NCX activity occurred without modification of NCX protein expression. Changes in the amount of protein would affect both Ca^{2+} efflux and influx mediated by NCX. Takimoto et al. reported that heterozygous NCX knockdown mice displayed improved systolic function and larger hypertrophic response to pressure overload that was attributed to lesser Ca^{2+} efflux [22]. Actually, NCX downregulation depressed the rate of $[Ca^{2+}]_i$ transient rise and decline, and it markedly elevated diastolic $[Ca^{2+}]_i$ in NRVMs [11].

Although simplified by the assumption that $[Na^+]_i$ and $[Ca^{2+}]_i$ transient were uniform throughout the cytosol, the estimation of E_{NCX} predicts that Ca^{2+} influx via NCX may occur in NRVMs under control conditions and that it may be substantially increased in the presence of ET-1 stimulation. However, there are probably spatial gradients for both $[Na^+]_i$ and $[Ca^{2+}]_i$ transient during the twitch with larger changes for both subsarcolemmal $[Na^+]_i$ and $[Ca^{2+}]_i$ than those sensed by the fluorescent indicators. Higher subsarcolemmal $[Na^+]_i$ would favor a more extended period for NCX_{rev} operation on the one hand. On the other hand, higher subsarcolemmal $[Ca^{2+}]_i$ may limit net Ca^{2+} entry via NCX. While the physiological role of Ca^{2+} entry via NCX is controversial in adult ventricular tissue [23], in neonatal cells where AP duration is longer (especially in rat) and NCX expression and current are higher [24,25], it may be of particular importance. It was reported that Ca^{2+} influx via the NCX during an AP can account for normal excitation–contraction coupling in newborn ventricular myocytes [26].

To our knowledge, this is the first demonstration that NHE-1 inhibition prevents ET-1-induced hypertrophy. This finding is consistent with the growing volume of data

regarding the ability of NHE-1 inhibition to prevent or even regress CH in other experimental models [8,9]. Despite this research attention, the mechanism involved in the antihypertrophic effect of NHE-1 inhibition is not completely elucidated. Increases in $[Na^+]_i$ have been previously associated with cell growth [27,28]. Our results demonstrate that NHE-1 activity was higher in ET-1-treated NRVMs and that the higher $[Na^+]_i$ level of these cells was normalized with HOE 642 suggesting the involvement of the antiporter in the rise of $[Na^+]_i$ in hypertrophied neonatal myocytes. Moreover, NHE-1 inhibition normalized the increase in total cytosolic $[Ca^{2+}]_i$ and the larger Ca^{2+} influx via the NCX_{rev} promoted by extracellular Na^+ removal in ET-1-treated NRVMs at the same time that it prevented the development of hypertrophy, strongly suggesting a link between both effects.

Elevation of $[Ca^{2+}]_i$ has been implicated in CH signaling. In this regard, ET-1 may act at several points of cell Ca^{2+} handling. ET-1 has been reported to elevate [29] as well as reduce [30] $[Ca^{2+}]_i$ in NRVMs. In our experimental conditions, an increase in total cytosolic $[Ca^{2+}]_i$ was observed. Also, the rise in $[Ca^{2+}]_i$ promoted by extracellular Na^+ removal was markedly increased in ET-1-treated NRVMs, effect that can be ascribed to the larger transarcolemmal Na^+ gradient driving the operation of NCX_{rev}. However, a Na^+-independent effect of ET-1 on NCX_{rev} activity cannot be completely ruled out [31,32]. We are aware that such a situation (extracellular Na^+ deprivation) is non-physiologic but a similar condition of V_m exceeding E_{NCX} and favoring NCX_{rev} mode due to elevated $[Na^+]_i$ level may well occur during the course of APs [20,33–36]. It may be argued that the extent of this period was estimated on the bases of a theoretical AP and a possible ET-1 effect on AP duration was not taken into account. It has been previously shown that ET-1 causes an increase in AP duration [36]. If this is the case, then the possibility of NCX_{rev} activity would be even larger than what was calculated here. The possibility that the increase in $[Na^+]_i$ level could have impaired Ca^{2+} efflux via the NCX was also considered [37]. However, it seems unlikely that this effect could have contributed to our results because no significant change in the relaxation of caffeine-evoked $[Ca^{2+}]_i$ transients was detected in hypertrophied NRVMs. Similarly, it was suggested that Na^+ influx may play a role in altering Ca^{2+} homeostasis, possibly through increasing NCX_{rev} in catecholamine-induced cardiac muscle hypertrophy, in which the rate of decline of caffeine-induced Ca^{2+} transients was not different from control [38].

We found that KB-R7943 decreased CSA in unstimulated NRVMs. The effect was not associated with a reduction in ^{3}H-phenylalananine incorporation or ANF mRNA expression suggesting that it was not due to a generalized decrease in cell growth. At present, we do not have an explanation for this but the fact that DMSO produced a similar effect raises the possibility of a non-specific action of the diluent.

In summary, our data represent the first evidence that NCX_{rev} is a Ca^{2+} entry pathway linked to ET-1-induced CH in NRVMs. Zhu et al. showed that ET-1 induces cardiomyocyte hypertrophy through the activation of CaMKII- and calcineurin-dependent pathways [39] and our study now identifies a novel pathway (NCX_{rev}) for the rise in $[Ca^{2+}]_i$ responsible for the activation of prohypertrophic intracellular signals. NHE-1 inhibitors by reducing the rise in $[Na^+]_i$ that favors NCX_{rev} inhibits the hypertrophic response. This does not deny the possibility that other signaling or Ca^{2+}-dependent pathways may also contribute to the development of CH. In connection with this, a recent report showed that $InsP_3$-dependent perinuclear Ca^{2+} release and CaMKII activation mediate ET-1-induced hypertrophy in adult cardiomyocytes [40]. Even though adult ventricular myocytes differ somewhat from cultured NRVMs, the latter undergo cellular responses that parallel many of the cellular changes seen in vivo in hypertrophying hearts. It would be therefore interesting in the future to corroborate to which extent the sequence of events described here occurs in the adult heart. Besides demonstrating that normalization of $[Na^+]_i$ level might be the mechanism underlying the prevention of CH development by NHE-1 inhibitors, the present results point to another potential pharmacological target, NCX_{rev}, to control myocardial hypertrophy.

Acknowledgments

This work was supported in part by grants PICT 12412, 12480 and 14565 to MCC de Hurtado, GEC de Cingolani and IL Ennis, respectively, and partly by grants PIP 02582 (MCC de Hurtado) and 02874 (GEC de Cingolani). Authors thank the gift of HOE 642 and TAK 044 kindly provided by Aventis Pharma and Takeda Pharmaceuticals Co., respectively.

References

[1] Levy D, Garrison RJ, Savage DD, Kannel WD, Castelli WP. Prognostic implications of echocardioghraphically determined left ventricular mass in The Framingham Heart Study. N Engl J Med 1990;322:16561–6.
[2] Sadoshima J, Xu Y, Slayter HS, Izumo S. Autocrine release of angiotensin II mediates stretch-induced hypertrophy of cardiac myocytes in vitro. Cell 1993;75:977–84.
[3] Ito H, Hirata Y, Adachi S, Tanaka M, Tsujino M, Koike A, et al. Endothelin-1 is an autocrine/paracrine factor in the mechanism of angiotensin II-induced hypertrophy in cultured rat cardiomyocytes. J Clin Invest 1993; 92:398–403.
[4] Liang F, Gardner DG. Autocrine/paracrine determinants of strain-activated brain natriuretic peptide gene expression in cultured cardiac myocytes. J Biol Chem 1998;273:14612–9.
[5] Kramer BK, Smith TW, Kelly RA. Endothelin and increased contractility in adult rat ventricular myocytes. Role of intracellular alkalosis induced by activation of the protein kinase C-dependent Na^+–H^+ exchanger. Circ Res 1991;68:269–79.
[6] Matsui H, Barry WH, Livsey C, Spitzer KW. Angiotensin II stimulates sodium–hydrogen exchange in adult rabbit ventricular myocytes. Cardiovasc Res 1995;29:215–21.
[7] Moor AN, Fliegel L. Protein kinase-mediated regulation of the Na(+)/H(+) exchanger in the rat myocardium by mitogen-activated protein kinase-dependent pathways. J Biol Chem 1999;274:22985–92.
[8] Cingolani HE, Camilión de Hurtado MC. Na^+–H^+ exchanger inhibition: a new antihypertrophic tool. Circ Res 2002;90:751–3.
[9] Fliegel L, Karmazyn M. The cardiac Na–H exchanger: a key downstream mediator for the cellular hypertrophic effects of paracrine, autocrine and hormonal factors. Biochem Cell Biol 2004;82:626–35.
[10] Pérez NG, Villa-Abrille MC, Aiello EA, Dulce RA, Cingolani HE, Camilión de Hurtado MC. A low dose of angiotensin II increases

inotropism through activation of reverse Na^+/Ca^{2+} exchange by endothelin release. Cardiovasc Res 2003;60:589–97.

[11] Hurtado C, Ander BP, Maddaford TG, Lukas A, Hryshko LV, Pierce GN. Adenovirally delivered shRNA strongly inhibits Na^+–Ca^{2+} exchanger expression but does not prevent contraction of neonatal cardiomyocytes. J Mol Cell Cardiol 2005;38:647–54.

[12] Ennis IL, Garciarena CD, Pérez NG, Dulce RA, Camilión de Hurtado MC, Cingolani HE. Endothelin isoforms and the response to myocardial stretch. Am J Physiol, Heart Circ Physiol 2005;288:H2925–30.

[13] Harootunian AT, Kao JPY, Eckert BK, Tsien RY. Fluorescence ratio imaging of cytosolic free Na^+ in individual fibroblasts and lymphocytes. J Biol Chem 1989;264:19449–57.

[14] Grynkiewicz G, Poenie M, Tsien RY. A new generation of Ca2+ indicators with greatly improved Fluorescence properties. J Biol Chem 1985;260: 3440–50.

[15] Bassani RA, Bassani JWM, Bers DM. Mitochondrial and sarcolemmal Ca2+ transport reduce $[Ca^{2+}]i$ during caffeine contractures in rabbit cardiac myocytes. J Physiol 1992;453:591–608.

[16] Yamazaki T, Komuro I, Kudoh S, Zou Y, Shiojima I, Hiroi Y, et al. Endothelin-1 is involved in mechanical stress-induced cardiomyocyte hypertrophy. J Biol Chem 1996;271:3221–8.

[17] Cullen JP, Bell D, Kelso EJ, McDermott BJ. Use of A-192621 to provide evidence for involvement of ET_B-receptors in endothelin-1-mediated cardiomyocyte hypertrophy. Eur J Pharmacol 2001;417:157–68.

[18] Mullan DM, Bell D, Celso EJ, McDermott BJ. Involvement of ETA and ETB receptors in the hypertrophic effects of ET-1 in rabbit ventricular cardiomyocytes. J Cardiovasc Pharmacol 1997;29:350–9.

[19] Slodinski MK, Blaustein MP. Na^+/Ca^{2+} exchange in neonatal rat heart cells: antisense inhibition and protein half-life. Am J Physiol, Cell Physiol 1998;275:459–67.

[20] Bers DM. Excitation–contraction coupling and cardiac contractile force. 2nd ed. Dordrecht: Kluwer Academic Publishers; 2001. p. 133–60. Chapter 6.

[21] Watano T, Kimura J, Morita T, Nakanishi H. A novel antagonist, No. 7943, of the $Na^+/Ca2^+$ exchange current in guinea-pig cardiac ventricular cells. Br J Pharmacol 1996;119:555–63.

[22] Takimoto E, Yao A, Toko H, Takano H, Shimoyama M, Sonoda M, et al. Sodium calcium exchanger plays a key role in alteration of cardiac function in response to pressure overload. FASEB J 2002;16:373–8.

[23] Satoh H, Ginsburg KS, Qing K, Terada H, Hayashi H, Bers DM. KB-R7943 block of Ca^{2+} influx via Na^+/Ca^{2+} exchange does not alter twitches or glycoside inotropy but prevents Ca^{2+} overload in rat ventricular myocytes. Circulation 2000;101:1441–6.

[24] Boerth SR, Zimmer DB, Artman M. Steady-state mRNA levels of the sarcolemmal Na^+–Ca^{2+} exchanger peak near birth in developing rabbit and rat hearts. Circ Res 1994;74:354–9.

[25] Artman M, Ichikawa H, Avkiran M, Coetzee WA. Na^+/Ca^{2+} exchange current density in cardiac myocytes from rabbits and guinea pigs during postnatal development. Am J Physiol 1995;268:H1714–22.

[26] Haddock PS, Coetzee WA, Cho E, Porter L, Katoh H, Bers DM, et al. Subcellular $[Ca^{2+}]i$ gradients during excitation–contraction coupling in newborn rabbit ventricular myocytes. Circ Res 1999;85:415–27.

[27] Kent RL, Hoober JK, Cooper IV G. Load responsiveness of protein synthesis in adult mammalian myocardium: role of cardiac deformation linked to sodium influx. Circ Res 1989;64:74–85.

[28] Huang L, Li H, Xie Z. Ouabain-induced hypertrophy in cultured cardiac myocytes is accompanied by changes in expression of several late response genes. J Mol Cell Cardiol 1997;29:429–37.

[29] Touyz RM, Fareh J, Thibault G, Tolloczko B, Lariviere R, Schiffrin EL. Modulation of Ca^{2+} transients in neonatal and adult rat cardiomyocytes by angiotensin II and endothelin-1. Am J Physiol, Heart Circ Physiol 1996; 270:H857–68.

[30] Kohmoto O, Ikenouchi H, Hirata Y, Momomura S, Serizawa T, Barry WH. Variable effects of endothelin-1 on $[Ca^{2+}]_i$ transients, pH_i, and contraction in ventricular myocytes. Am J Physiol, Heart Circ Physiol 1993;265: H793–800.

[31] Ballard C, Schaffer S. Stimulation of the Na^+/Ca^{2+} exchanger by phenylephrine, angiotensin II and endothelin 1. J Mol Cell Cardiol 1996;28:11–7.

[32] Aiello EA, Villa-Abrille MC, Dulce RA, Cingolani HE, Pérez NG. Endothelin-1 stimulates the Na^+/Ca^{2+} exchanger reverse mode through intracellular Na^+ (Na_i^+)-dependent and Na_i^+-independent pathways. Hypertension 2005;45:288–93.

[33] Armoundas AA, Hobai IA, Tomaselli GF, Winslow RL, O'Rourke B. Role of sodium–calcium exchanger in modulating the action potential of ventricular myocytes from normal and failing hearts. Circ Res 2003; 93:46–53.

[34] Waisser-Thomas J, Piacentino III V, Gaughan JP, Margulies K, Houser SR. Calcium entry via Na/Ca exchange during the action potential directly contributes to contraction of failing human ventricular myocytes. Cardiovasc Res 2003;57:974–85.

[35] von Lewinski D, Stumme B, Maier LS, Luers C, Bers DM, Pieske B. Stretch-dependent slow force response in isolated rabbit myocardium is Na^+ dependent. Cardiovasc Res 2003;57:1052–61.

[36] Yorikane R, Koike H, Miyake S. Electrophysiological effects of endothelin-1 on canine myocardial cells. J Cardiovasc Pharmacol 1991;17:S159–62.

[37] Baartscheer A, Schumacher CA, Belterman CNW, Coronel R, Fiolet JWT. $[Na^+]_i$ and the driving force of the Na^+/Ca^{2+}-exchanger in heart failure. Cardiovasc Res 2003;57:986–95.

[38] Chorvatova A, Hart G, Hussain M. Na^+/Ca^{2+} exchange current ($I_{Na/Ca}$) and sarcoplasmic reticulum Ca^{2+} release in catecholamine-induced cardiac hypertrophy. Cardiovasc Res 2004;1:278–87.

[39] Zhu W, Zou Y, Shiojima I, Kudoh S, Aikawa R, Hayashi D, et al. Ca^{2+}/calmodulin-dependent kinase II and calcineurin play critical roles in endothelin-1-induced cardiomyocyte hypertrophy. J Biol Chem 2000; 275:15239–45.

[40] Wu X, Zhang T, Bossuyt J, Li X, McKinsey TA, Dedman TR, et al. Local InsP3-dependent perinuclear Ca^{2+} signaling in cardiac myocyte excitation-transcription coupling. J Clin Invest 2006;116:675–82.